Multichromophoric Dendrimers as Single-Photon Sources: A Single-Molecule Study

Sadahiro Masuo,[†] Tom Vosch,[†] Mircea Cotlet,[†] Philip Tinnefeld,[‡] Satoshi Habuchi,[†] Toby D. M. Bell,[†] Ingo Oesterling,[§] David Beljonne,[||] Benoît Champagne,[⊥] Klaus Müllen,[§] Markus Sauer,[‡] Johan Hofkens,*[,†] and Frans C. De Schryver*[,†]

Department of Chemistry, Katholieke Universiteit Leuven, Celestijnenlaan 200F, 3001 Heverlee, Belgium, Fakultät für Physik, Angewandte Laserphysik and Laserspektroskopie, Universität Bielefeld, Universitätsstr. 25, 33615 Bielefeld, Germany, Laboratory for Chemistry of Novel Materials, University of Mons-Hainaut, 20 Place du Parc, B-7000 Mons, Belgium, Laboratoire de Chimie Théorique Appliquée, Facultés Universitaires Notre-Dame de la Paix (FUNDP), Rue de Bruxelles, 61, B-5000 Namur, Belgium, and Max-Planck-Institut für Polymerforschung, Ackermannweg 10, 55128 Mainz, Germany

Received: May 21, 2004; In Final Form: August 3, 2004

Single-molecule fluorescence spectroscopy was performed on a number of multi-peryleneimide substituted polyphenylene dendrimers for the purpose of investigating the parameters which influence the efficiency of the dendrimers as single-photon sources at room temperature. Analysis of fluorescence intensity, lifetime, and interphoton arrival time distribution revealed that all measured first-generation dendrimers behave as single-photon emitters when more than one chromophore is excited by a single excitation pulse regardless of the number of constituent chromophores. This is a result of efficient singlet−singlet annihilation, which becomes less efficient in higher-generation dendrimers when the interchromophoric distance increases. The efficiency of the investigated dendrimers as single-photon sources depends on several other parameters, such as the nature of the surrounding polymer matrix, the number of chromophores, and the extent of interchromophoric interactions. These parameters mainly affect the frequency of singlet−triplet annihilation, which in turn dominates the quality of these multichromophoric dendrimers as single-photon sources. The results reported here are important not only for the design of single-photon sources based on single organic molecules but also for a fundamental understanding of natural and artificial multichromophoric systems.

Introduction

The generation of nonclassical states of light[1] is of fundamental scientific and technological interest and has attracted much attention in the past few years. Nonclassical states exhibit sub-Poissonian or "squeezed" statistics,[2] while photons from classical light sources follow Poissonian statistics or super-Poissonian statistics. Deterministic single-photon sources exhibit nonclassical behavior in that they produce light pulses containing one photon per pulse *at a user-specified time*. The desire to realize controllable single-photon sources is driven mainly by potential applications in quantum cryptography[3−5] and certain quantum computational problems.[6] For example, perfect security of quantum cryptography can be realized if each bit of information is encoded on a single photon.[3]

A single-photon source was first observed in the resonance fluorescence of sodium atoms in a low-density atomic beam.[7] More recently, various experiments have been proposed to create a single-photon source, for example, involving optically[8−10] or electronically[11] excited semiconductor nanostructures or optically excited single molecules either by laser[12] or through rapid adiabatic passage.[13] Because these experiments have to be performed at cryogenic temperatures, the detection efficiency is limited to 10^{-3}−10^{-4}. Another approach is to generate single-photon sources at room temperature. In this case, a higher detection efficiency (∼0.1) can be achieved. Such sources rely on nitrogen-vacancy color centers in a diamond crystal,[14] CdSe quantum dots,[15] or on emission from single molecules excited by a pulsed laser.[16−20] When the pulse repetition period is much longer than the fluorescence lifetime and the pulse duration is much shorter than the fluorescence lifetime, a single molecule can emit only one photon per excitation pulse.

Our experimental realization of a deterministic single-photon source is based on pulsed laser excitation of single multichromophoric dendrimers which are decorated with peryleneimide chromophores embedded in a thin polymer matrix. Peryleneimide is a well-known chromophore that is well suited for single-molecule spectroscopy because of its high photostability, molar absorption coefficient ($\epsilon = 38\,000\ M^{-1}\ cm^{-1}$ at 490 nm), and fluorescence quantum yield ($\Phi_f = 0.95$ in toluene).[21] Recently, we have demonstrated that individual bi- and tetrachromophoric dendrimers emit only one photon per excitation pulse even when more than one chromophore was excited by a laser pulse.[16,21] This behavior results from efficient singlet−singlet annihilation (S_1−S_1 annihilation),[22] which is the key process and main advantage of the use of multichromophoric dendrimers as single-photon sources as the absorption cross section can be increased easily with the number of chromophores. By increasing the number of chromophores, multichromophoric dendrimers can reach higher count rates of fluorescence at a lower excitation power (vide infra) and achieve longer survival times as a single-photon source compared to single chromophoric molecules.

* To whom correspondence should be addressed. Tel.: +32 (0) 16 327 405. Fax: +32 (0) 16 327 989. E-mail: johan.hofkens@chem.kuleuven.ac.be (J.H.); frans.deschryver@chem.kuleuven.ac.be (F.C.D.S.).
[†] Katholieke Universiteit Leuven.
[‡] Universität Bielefeld.
[§] Max-Planck-Institut für Polymerforschung.
[||] University of Mons-Hainaut.
[⊥] Facultés Universitaires Notre-Dame de la Paix (FUNDP).

10.1021/jp047804b CCC: $27.50
Published on Web 10/06/2004

Multichromophoric systems, however, often show triplet blinking,[21−25] as observed for other single organic molecules.[26,27] For multichromophoric molecules, triplet blinking is understood as follows. After excitation, one of the chromophores undergoes intersystem crossing to an excited triplet state, T_1. When another chromophore is then excited by the next excitation pulse, an excited singlet state, S_1, and an excited triplet state, T_1, are present simultaneously in the same multichromophoric molecule. If the triplet state exhibits transitions into higher excited triplet states, T_n, that are in resonance with the $S_1 \rightarrow S_0$ transition, singlet−triplet energy transfer, that is, energy transfer from the excited singlet state to the energetically lower lying triplet state, can occur. This process is called singlet−triplet annihilation (S_1-T_1 annihilation) and is an undesirable process in single-photon sources because it quenches photon emission. The above-mentioned S_1-S_1 and S_1-T_1 annihilation processes are Förster type fluorescence resonance energy transfer processes; that is, their efficiency depends on the distance between the interacting chromophores, the relative orientation of their transition dipoles, and their spectral properties. These two processes are the key mechanisms affecting the single-photon-source performance of multichromophoric dendrimers, and the understanding and control of these mechanisms are crucial for the realization of better single-photon sources. As a result of the tunability of the number of chromophores, the size, and the structure of polyphenylene dendrimers, the systems allow the investigation of the influence of interchromophoric distance and interaction and the number of chromophores on the efficiency of S_1-S_1 and S_1-T_1 annihilation. Interchromophoric interactions present in multichromophoric dendrimers can be described either by weak coupling of the chromophores using Förster theory or stronger coupling where the Förster model is not applicable.

In this paper, we investigate the parameters which influence the efficiency of multichromophoric dendrimers as single-photon sources by monitoring the fluorescence intensity, fluorescence decay time, and interphoton arrival time distribution (coincidence of antibunching measurements); specifically, the influences of the (1) interchromophoric distance, (2) polymer matrix, (3) the number of chromophores (within the Förster limit), and (4) interchromophoric interaction (weak coupling and stronger coupling) are studied. The results obtained are important not only for the realization of an efficient room-temperature single-photon source but also for a better understanding of the photophysical properties of multichromophoric systems such as light harvesting antennae,[28,29] oligomeric fluorescent proteins,[30] and conjugated polymers.[31−33]

Experimental Section

To investigate the influence of the parameters on the efficiency of multichromophoric dendrimers as a single-photon source, three rigid multichromophoric dendrimers with well-defined structures were chosen: a first-generation tetrachromophoric dendrimer, g1r4, (g1, first generation; r4, four chromophores, each connected at the para position of the phenyl at the rim of each of the four rigid polyphenylene arms substituting a sp^3 hybridized central carbon atom), an extended tetrachromophoric dendrimer eg1r4, and a first generation octachromophoric g1r8. In addition, a first-generation monochromophoric dendrimer, g1r1, was measured as a model compound for comparison. The chemical structures of the dendrimers are shown in Figure 1, and syntheses of the dendrimers are described elsewhere.[34−38] To estimate the interchromophoric distances in these dendrimers, energetically optimized chemical structures were calculated using the Merck molecular force field algorithm in SPARTAN. This algorithm has proven to be quite successful for determining equilibrium geometries and, in particular, equilibrium conformations. From the optimized structures, center-to-center interchromophoric distances were calculated (Table 1). It is known that as a result of the synthetic route in the eg1r4 dendrimer, a large number of isomers with different chromophore arrangements are present.

The value in Table 1 of the interchromophoric distance in eg1r4 relates to the isomer shown in Figure 1. As can be observed from the chemical structure of g1r8, the interchromophoric distances will be different for the chromophores within one branch and between two branches; thus, both the interchromophoric distance for the closest pair and the average of the other pairs are shown in Table 1.

The interchromophoric distances in g1r4 and eg1r4 would suggest that the interchromophoric interactions are limited to the weak coupling limit (Förster regime), and this is supported by absorption and fluorescence spectra in solution and by the fluorescence decays at the single-molecule level which do not give any indications of strong coupling (vide infra). In contrast, the chromophores in g1r8 are spatially much closer leading to stronger coupling interactions between them.

Because it was experimentally not possible to determine the position of the triplet state, theoretical calculations were performed. The structures of the singlet ground state and lowest-lying triplet state of peryleneimide were optimized using Kohn−Sham density functional theory[39] with the B3LYP exchange-correlation function[40] and the 6-31G* basis set as implemented in the Gaussian 98 program. The adiabatic S_0-T_1 excitation energy was evaluated from their energy difference. A value of 905 nm was found.

Samples were prepared by spin-coating chloroform (Sigma-Aldrich, spectrophotometric grade) solutions of 10 mg/mL poly(methyl methacrylate) (PMMA) or zeonex containing $\sim 10^{-10}$ M of the different dendrimers onto carefully cleaned glass coverslips at 1500 rpm for 60 s yielding polymer films of ~100-nm thickness (checked by atomic force microscopy measurements).

For single-molecule measurements, a classical Hanbury−Brown and Twiss type coincidence setup[41] in combination with pulsed laser excitation was used. Details of the setup are given elsewhere.[42] Briefly, as an excitation light source, the frequency doubled output of a Ti:sapphire laser (Tsunami, Spectra Physics, 488 nm, 8.18 MHz, 1.2 ps full width at half-maximum) was rendered circularly polarized by a $\lambda/4$ waveplate and then coupled into a microscope (objective: Olympus, 1.4 NA, 60×). The fluorescence from single dendrimer molecules was collected by the same objective, split by a 50/50 nonpolarizing beam splitter and detected by two avalanche photodiodes (APD, SPCM15, EG&G, Quebec). The signals from both APDs were fed into the router of a time-correlated single-photon-counting computer interface board (SPC-630, Becker & Hickl), and the laser synchronization signal was connected to the synchronization input of the board. The signal from one of the two APDs was delayed using a delay generator to compensate for the dead time of the SPC board. Time-resolved data were acquired using the first-in-first-out mode in which the arrival time after the beginning of the acquisition, the time delay between the start and stop pulse, and the detection channel (APD1 or APD2) are registered for each detected fluorescence photon. A LabView routine was written to obtain the appropriate signature of antibunching and the fluorescence decay time, allowing histograms of the interphoton arrival times and time-resolved fluorescence decays to be constructed. All measurements were performed at room temperature.

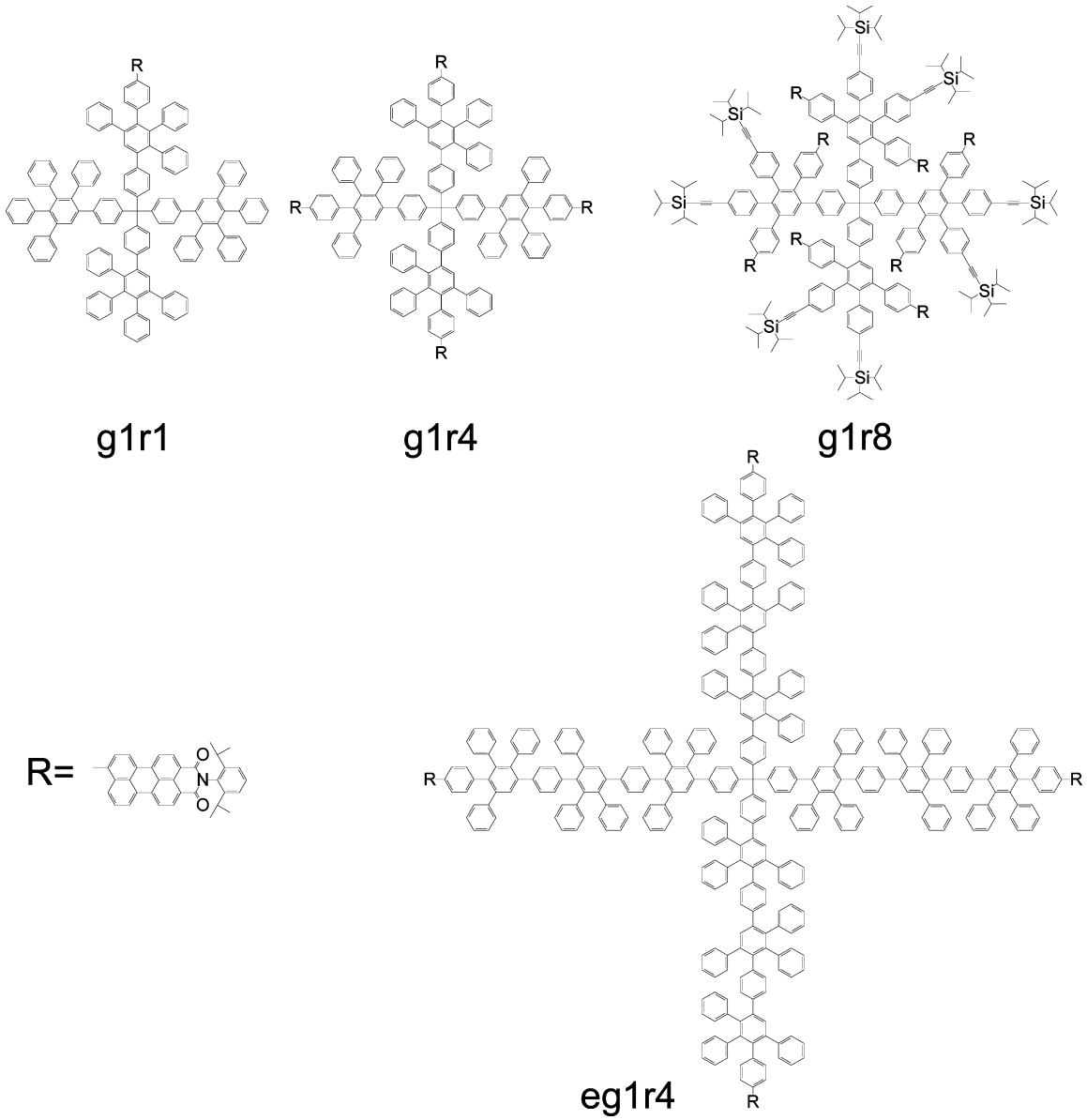

Figure 1. Chemical structures of three multichromophoric dendrimers g1r4, eg1r4, and g1r8 and the single chromophoric model dendrimer g1r1.

TABLE 1: Calculated Interchromophoric Distances (Center-to-Center) of Multichromophoric Dendrimers

	distance		distance	
glr4	2.7 nm	glr8	0.8 nm	2.3 nm
eg1r4	6.0 nm			

Results and Discussion

Steady-state absorption and fluorescence spectra of g1r4 and g1r8 dissolved in toluene are shown in Figure 2. Absorption and fluorescence spectra of g1r4 are identical to those of the single chromophoric dendrimer, g1r1, indicating the absence of strongly coupled interchromophoric interactions. On the other hand, stronger interchromophoric interaction can be seen in g1r8. The absorption spectrum of g1r8 is slightly broader than that of g1r4, although the values of the wavelengths of the two maxima are exactly the same as for g1r4. This broadening is attributed to interchromophoric interaction in the ground state. In addition, the fluorescence spectrum of g1r8 is quite different compared to that of g1r4, showing red-shifted, broader, less structured fluorescence. This fluorescence spectrum is attributed to excimer-like emission from ground-state interacting chromophores as a result of the shorter interchromophoric distances in g1r8 compared to those of g1r4 (Table 1).

The transient S_1-S_n and T_1-T_n absorption spectra of g1r1 in toluene are shown in Figure 2b,c, respectively. To show the spectral overlap clearly, the emission spectrum of g1r4 is also shown in both figures. The rate constants of energy hopping (k_{hop}) and S_1-S_1 annihilation (k_{anni}) for g1r4 were determined by a time-resolved fluorescence depolarization experiment[43] and femtosecond transient absorption spectroscopy[44] or fluorescence upconversion,[45] respectively. A value of 4.6×10^9 s^{-1} was obtained for k_{hop} while the rate constant for S_1-S_1 annihilation, k_{anni}, was estimated as 1.0×10^{11} s^{-1}. The R_0 of S_1-S_1 annihilation was calculated to be 7.35 nm by using the following expression based on a value of 4.4 nm for the R_0 of energy hopping where τ_D is the fluorescence lifetime of the donor in absence of the acceptor.

$$\frac{k_{hop}}{k_{anni}} = \frac{1/\tau_D[R_{0(hop)}/R]^6}{1/\tau_D[R_{0(anni)}/R]^6} \quad (1)$$

The excitation power dependence of the fluorescence count rate measured from a single g1r4 embedded in a PMMA film

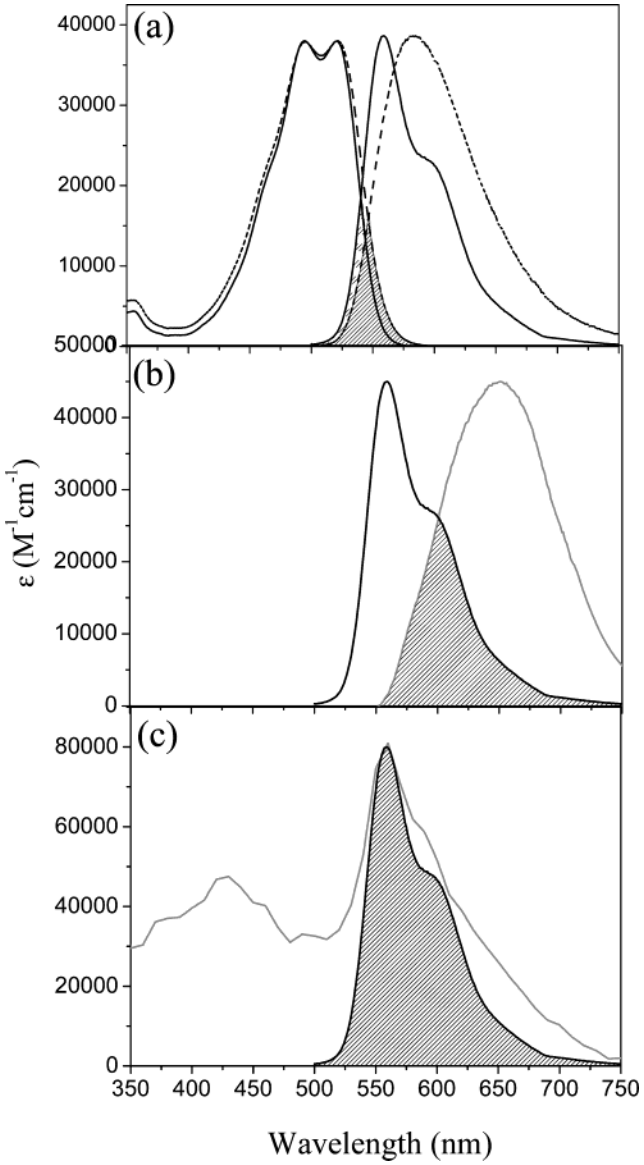

Figure 2. (a) Steady-state absorption and fluorescence spectra of g1r4 (solid lines) and g1r8 (dotted lines) in toluene. (b) Transient singlet−singlet (S_1-S_n) absorption (gray line) and fluorescence spectra of g1r4 (solid line) in toluene. (c) Transient triplet−triplet (T_1-T_n) absorption (gray line) and fluorescence spectra of g1r4 (solid line) in toluene. The shaded areas indicate the spectral overlap. The extinction coefficients of the different absorption spectra are indicated on the left axis, and the fluorescence spectra are normalized to the peak extinction coefficient to illustrate the change in overlap.

is shown in Figure 3 together with that of g1r1 for comparison. For the case of g1r4, the fluorescence count rate was estimated from the first intensity level because fluorescence intensity traces of the single multichromophoric dendrimers show several intensity levels attributed to successive photobleaching of individual chromophores, and the laser power was measured before it was introduced to the microscope. For comparison, data were fitted by the saturation law of a two-level system.[18,19]

$$I_F = \frac{I_{sat}(P/P_{sat})}{1 + P/P_{sat}}[1 - \exp\{-(1 + P/P_{sat})\tau_P/\tau_D\}] \qquad (2)$$

Here, I_{sat} is the count rate of saturated fluorescence, P and P_{sat} are the laser power and saturation power, respectively, and τ_p and τ_D are the pulse width and fluorescence lifetime, respectively. Note that this formula is an approximation, only valid

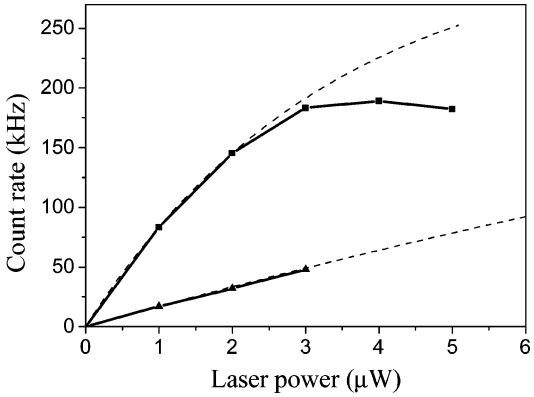

Figure 3. Excitation laser power dependence of the fluorescence count rate measured from a single g1r4 (solid line with square) and g1r1 (solid line with triangle) embedded in PMMA, and saturation curves calculated from a two-level model (dotted lines).

for short pulse durations. It can be seen that the fluorescence count rate of g1r4 saturates for laser powers over 3 μW and is not well fitted by the two-level model. All measured multichromophoric dendrimers showed such a saturation behavior within the same laser power range. The fluorescence count rate of g1r1 does not saturate at this excitation power regime. On the basis of the data reported in Figure 3, it is expected that the fluorescence count rate of g1r1 can reach its maximum at a few tens of microwatts. The excitation probability of g1r4 for the case of the 4-μW laser power was calculated as follows. The energy per pulse of 4.89×10^{-13} J is given by dividing 4 μW or 4×10^{-6} J/s by 8.18×10^6 pulses/s (laser repetition rate being 8.18 MHz). This energy corresponds to 1.20×10^6 photons per pulse for photons of 488-nm wavelength. The diffraction-limited focal point has an area of 3.1×10^{-10} cm^2 resulting in a density of 3.87×10^{15} photons/cm^2. The absorption cross section of g1r4 is 5.81×10^{-16} cm^2, and multiplication of the photon density with the absorption cross section yields a value of 2.2. This value indicates the possibility of two chromophore excitations per single excitation pulse. It is considered, therefore, that the measured saturation behavior is due to S_1-S_1 annihilation as a result of two chromophore excitations per pulse at the first intensity level, and it can be seen that multichromophoric dendrimers can reach their maximum fluorescence count rates at lower excitation power compared to single chromophoric systems. For all coincidence measurements, excitation laser powers of 3−5 μW were used to increase the probability that two or more chromophores are excited at the same time.

Coincidence Measurements for the Dendrimers Having Four Peryleneimide Chromophores. The time traces of the fluorescence intensity, the fluorescence decay time, and the interphoton arrival time distribution, measured from a g1r4 molecule embedded in zeonex film, are shown in Figure 4. In addition, the time trace of the ratio of the central peak (N_C) to the average of the lateral peaks (N_L), that is, N_C/N_L, is given in Figure 4b. Several intensity levels in the fluorescence intensity time trace (Figure 4b) indicate successive photobleaching of individual chromophores. As can be seen in Figure 4a, the fluorescence decay time shows a constant value of around 4 ns which is characteristic of peryleneimide. Thus, the decay time trace indicates the absence of stronger interchromophoric interactions in g1r4. Figure 4c shows the interphoton arrival time distribution taken from the first intensity level of the time trace of g1r4 in Figure 4b, and Figure 4d shows an attenuated excitation laser beam (Ti:sapphire laser) that had approximately the same count rate. The center peak of the distribution at the time, $t = 0$ ns, corresponds to photon pairs induced by the same

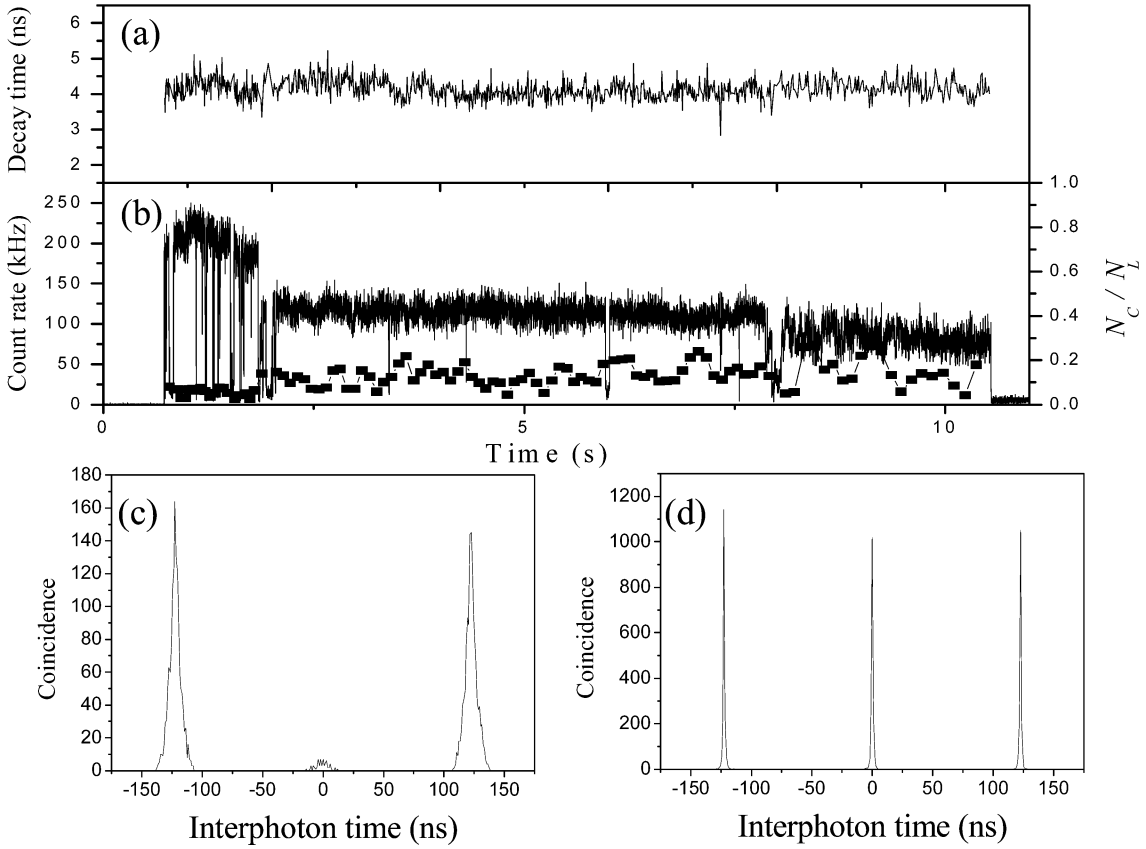

Figure 4. Typical time traces of fluorescence intensity (b, solid line), fluorescence decay time (a), and the ratio of the central peak to the average of the lateral peaks (N_C/N_L; b, squares) measured from a single g1r4 embedded in zeonex. (c) Interphoton arrival time distribution obtained from the first fluorescence intensity level of the time trace in panel b. (d) Interphoton arrival time distribution measured from an attenuated Ti:sapphire laser.

excitation laser pulse. In all other cases, interphoton arrival times are distributed around a multiple of the laser repetition period; that is, the peak appears every 122 ns. The peak width is determined by the fluorescence lifetime, and it can be seen that the peak width of g1r4 is broader than that of the pulsed laser beam. It has been shown, previously,[17] that the N_C/N_L ratio can be used to estimate the number of independently emitting chromophores. Neglecting background, N_C/N_L values of 0.0 and 0.5 are expected for one and two emitting chromophores, respectively. For the distribution shown in Figure 4c, N_C and N_L are 66 and 1376.5, respectively, giving a N_C/N_L value of 0.05. This indicates that g1r4 behaves as a single-photon emitter as the signal-to-background ratio means that the coincidences in the center peak can be attributed to background−background and background−signal photon pairs.[42] On the other hand, as can be seen in Figure 4d, the central peak of the interphoton arrival time distribution taken from the attenuated Ti:sapphire laser is identical in intensity to the lateral peaks. This distribution indicates typical Poissonian light behavior. A step-by-step analysis of the N_C/N_L ratio calculated every 20 000 photons is shown in Figure 4b. The consistently low value of the ratio proves that g1r4 behaves as a single-photon emitter throughout the trace.

The Mandel parameter, Q,[46,47] can be used to evaluate quantitatively the degree of deviation from Poissonian statistics and the efficiency of a single-photon source.

$$Q = (\sigma^2 - n_{av})/n_{av} \tag{3}$$

Here, σ^2 is the variance and n_{av} is the average number of detected photons per pulse. For the case of Poissonian light, Q should be 0 because σ^2 and n_{av} are equal. As σ^2 decreases, that is, for sub-Poissonian light, Q becomes negative, and for the case of a perfect single-photon source (one photon is produced by every excitation pulse), Q is -1 because a perfect single-photon source has $\sigma^2 = 0$. The Mandel parameter was calculated for a period of 366 ms in the first intensity level of g1r4 shown in Figure 4(b). This period includes 3.0×10^6 excitation pulses, and 77 598 photons were detected from 77 534 one-photon detection events and 32 two-photon detection events. From these values, the one-photon detection probability $P(1) = 0.0258$, the two-photon detection probability $P(2) = 1.07 \times 10^{-5}$, and $n_{av} = 0.0259$ were obtained. For an attenuated laser pulse with similar n_{av} of 0.0244, values for $P(1) = 0.0240$ and $P(2) = 1.71 \times 10^{-4}$ were obtained. Thus, the $P(2)$ of g1r4 is 16 times lower than that of a laser beam, that is, Poissonian light. The Mandel parameter for the time trace of g1r4 shown in Figure 4b was calculated to be $Q_d = -0.0270$ for the detected photons. Taking into account the detection efficiency of ~5%, the Mandel parameter of $Q_s = -0.519$ was obtained for the emitted photons. These values show that g1r4 behaves as a sub-Poissonian light source. The best value obtained of Q_s for g1r4 embedded in zeonex was $Q_s = -0.851$, a value which is close to that for a perfect single-photon source. An average value of $Q_s = -0.542$ was calculated from the first intensity level of 50 individual g1r4 molecules embedded in zeonex. For the monochromophoric dendrimer, g1r1, embedded in zeonex, measured under ambient conditions, and using the same excitation laser power, a value of $Q_s = -0.094$ was calculated. Values of Q_s for g1r1 and g1r4 are shown in Table 2. This low efficiency of g1r1 as a single-photon source results from the nonsaturated fluorescence at this excitation power.

TABLE 2: Triplet Lifetimes (τ_t), Triplet Formation Yields (Y_{tf}), and Mandel Parameters of g1r1 and g1r4, under Different Conditions (Embedded in PMMA under Ambient Condition and in Zeonex under Ambient Condition and N_2 Flow Condition Using Pulsed Excitation)[a]

compound	polymer	condition	τ_1 (ms)	Y_{tf}	Mandel parameter (Q_s)
g1r1	PMMA	ambient	0.37	1×10^{-4}	−0.071
	zeonex	ambient			−0.094
	zeonex	N_2	1.05	2×10^{-5}	
g1r4	PMMA	ambient	0.12	5×10^{-4}	−0.364
	zeonex	ambient			−0.542
	zeonex	N_2	0.40	7×10^{-4}	−0.378

[a] The same excitation power was used in all the experiments. Each value was calculated from the first intensity level of their fluorescence time traces as the average value of 50 individual molecules. A detection efficiency of 5% was taken into account.

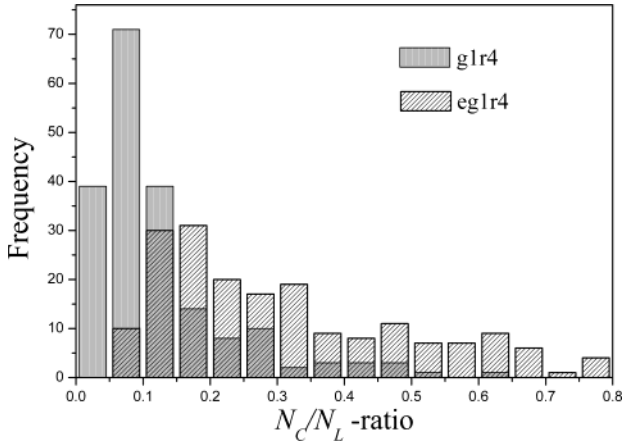

Figure 5. Histogram of the N_C/N_L ratio obtained from the first intensity level of 194 g1r4 and 189 eg1r4 molecules.

Influence of the Interchromophoric Distance in Dendrimers with Four Peryleneimide Chromophores. As described above, excitation energy transfer strongly depends on the interchromophoric distance, the orientation of the transient dipoles, and the spectral overlap. Here, we demonstrate that the influence of the interchromophoric distance on the S_1-S_1 annihilation can be examined by comparison of g1r4 and eg1r4. The interchromophoric distances calculated from the optimized structures of g1r4 and eg1r4 are shown in Table 1. For the isomer of eg1r4 depicted in Figure 1, the estimated interchromophoric distance is two times larger than that of g1r4. The efficiency of S_1-S_1 annihilation is determined by calculating N_C/N_L from the measured interphoton arrival time distribution. The histograms of the N_C/N_L values obtained from the first intensity level of g1r4 and eg1r4 are shown in Figure 5. These histograms are constructed from 194 molecules for g1r4 and 189 molecules for eg1r4. The ratios obtained from g1r4 show a narrower distribution than those for eg1r4 with an average N_C/N_L value for g1r4 of 0.1. This distribution indicates that efficient S_1-S_1 annihilation occurs in g1r4 as described above. On the other hand, the N_C/N_L values obtained from eg1r4 show a broader distribution ranging from 0.05 to 0.8, with an average ratio of 0.3. This indicates that the average efficiency of S_1-S_1 annihilation in eg1r4 is lower than for g1r4 and that some molecules do not behave as a single-photon emitter. The efficiency of S_1-S_1 annihilation estimated from the interchromophoric distance of the eg1r4 isomer depicted in Figure 1 is about 70% assuming a κ^2 of 1.92,[21] while that of g1r4 is 100%. Thus, it is anticipated that some isomers have less favorable orientations/distances between the chromophores resulting in inefficient S_1-S_1 annihilation. These results clearly show the influence of the interchromophoric distance on the S_1-S_1 annihilation efficiency.

Influence of Singlet−Triplet Annihilation on the Single-Photon Source. *(a) Influence of the Polymer Matrix on Singlet−Triplet Annihilation.* As a result of efficient S_1-T_1 annihilation, triplet blinking is prominent in these multichromophoric dendrimers. Although the efficiency of triplet formation of peryleneimide is small due to the low-lying triplet, triplet blinking remains nevertheless an undesirable process for a single-photon source because the singlet excited state is quenched by molecules in the triplet state, resulting in a loss of fluorescence. The off time due to triplet blinking, that is, the time a molecule spends in the triplet state, can be influenced by controlling the triplet decay time (τ_t), for example, by controlling the concentration of the efficient triplet quencher oxygen. Here, we discuss the influence of off times due to triplet blinking on a single-photon source by changing the polymer matrix and by flowing nitrogen over the sample to reduce the oxygen concentration. Fluorescence intensity time traces of g1r4 embedded in PMMA and in zeonex under ambient conditions and in zeonex under nitrogen flow are shown in Figure 6. The bin time of all the time traces is 0.2 ms.

Figure 6a shows that g1r4 embedded in PMMA under ambient conditions spends a considerable amount of time in the triplet state. Changing the polymer matrix to zeonex has a large impact on the triplet blinking as exemplified in Figure 6b, where only a few off states are visible for the entire time trace. This apparent lower frequency of off states most likely results from quenching by oxygen. For example, the oxygen permeability constant of PMMA is 20 times lower than that of low-density polyethylene, which we assume has a similar oxygen permeability as zeonex.[48] Therefore, shortening of τ_t leads to a lower observed frequency of off states. The off state can be visualized again upon flowing nitrogen over the sample (Figure 6c). The increase of the visible off state under nitrogen flow in the same polymer matrix evidences that the observed off states can directly be attributed to triplet blinking. The average τ_t and the triplet formation yield (Y_{tf}) calculated from 50 individual molecules are shown in Table 2.

Y_{tf} was calculated from the on time, τ_{on}, the initial fluorescence intensity, I_f, the fluorescence quantum yield, Φ_f (1 for all dendrimers), and the overall detection efficiency, Φ_{det}, which is approximately 0.05 for our experimental setup ($Y_{tf} = \Phi_f\Phi_{det}/\tau_{on}I_f$). τ_{on} and τ_t were estimated by building up the second-order intensity correlation (autocorrelation) from the fluorescence intensity traces.[49] For g1r1 and g1r4 in zeonex under ambient conditions, no value could be determined because of the fast quenching of the triplet state by oxygen. It can be seen that τ_t in zeonex under N_2 flow is longer than in PMMA under ambient conditions and Y_{tf} is influenced slightly. These calculated values quantitatively show that τ_t is controlled by the oxygen concentration. To evaluate the influence of the off time due to triplet blinking on the performance of g1r4 as a single-photon source, the Mandel parameters were calculated for the samples above (Table 2). It can be seen that the Mandel parameter of g1r4 in PMMA and in zeonex under N_2 flow is less negative compared to the value in zeonex under ambient conditions. This result indicates clearly that quenching of S_1 by T_1 in g1r4 results in a lower efficiency as a single-photon source and that the number of emitted photons is reduced by up to 30% due to triplet blinking. The effect is less pronounced in g1r1 (vide infra). High oxygen concentration conditions, such as in zeonex, are required to realize an efficient single-photon

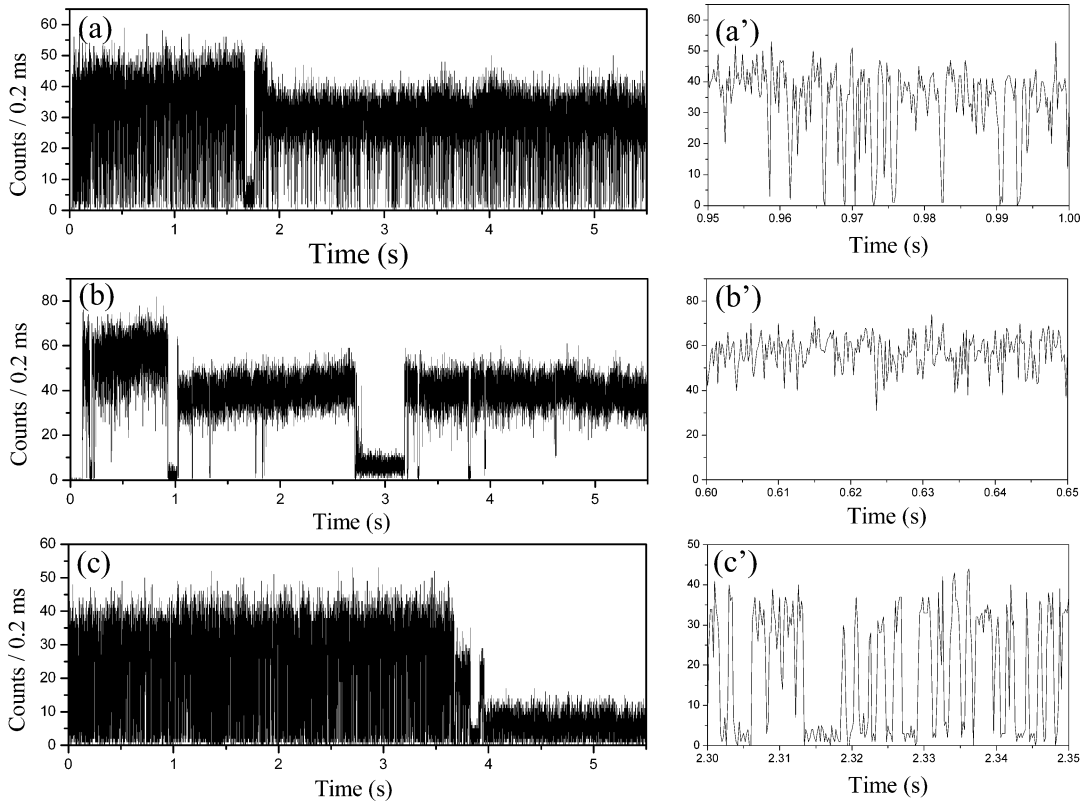

Figure 6. Fluorescence intensity time traces and expanded views of a g1r4 embedded in PMMA under ambient condition (a, a′), in zeonex under ambient condition (b, b′), and in zeonex under N_2 flow (c, c′).

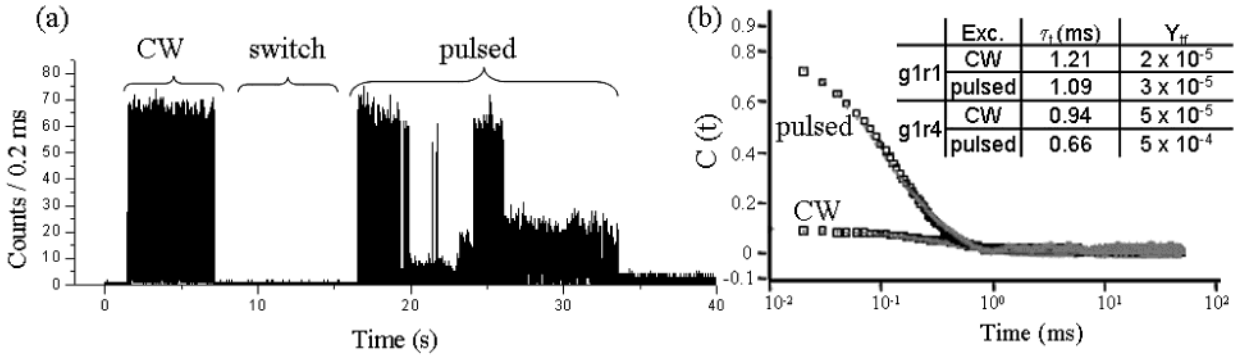

Figure 7. (a) Fluorescence intensity time trace of the same individual g1r4 molecule measured by CW excitation and pulsed excitation, with the same excitation power, embedded in PMMA under N_2 flow. From 7 to 16 s, the excitation source was switched from CW to pulsed excitation. (b) Autocorrelation curves built from the CW excitation period and the first intensity level of the pulsed excitation period in the time trace a. The average triplet lifetime (τ_t) and triplet formation yield (Y_{tf}) of g1r1 and g1r4 calculated from the CW excitation period and from the first intensity level of the pulsed excitation periods for about 40 molecules, respectively, are shown in the inset in part b.

source. However, longer off states compared to triplet blinking can sometimes be seen (for example, around 1 s in Figure 6b). These off states are attributed to other quenching species and will be discussed later.

(b) Influence of the Number of Chromophores on the Singlet−Triplet Annihilation Process in Weakly Coupled Systems. It has been observed recently that triplet formation and τ_t strongly depend on the number of chromophores.[50] Here, we demonstrate the influence of the number of chromophores on the S_1-T_1 annihilation process. Table 2 shows that Y_{tf} calculated from the first intensity levels increases with the number of chromophores (g1r4 > g1r1), while τ_t decreases with the number of chromophores (g1r4 < g1r1). Weak coupling of the chromophores in the rigid g1r4 molecules implies that the relative energies of the singlet and triplet states of individual chromophores are unaltered. Recently, it has been shown[21,50] by measuring under pulsed and continuous wave (CW) excitation conditions that the triplet parameters depend on the photon flux of the excitation process. The fluorescence intensity trace of a single g1r4 molecule embedded in PMMA under N_2 flow measured by both CW and pulsed excitation of the same laser power is shown in Figure 7a. Autocorrelation curves obtained from the fluorescence intensity trace with a CW excitation period and from the first intensity level with pulsed excitation are shown in Figure 7b.

In Figure 7a, a g1r4 molecule was first excited by a CW laser for several seconds, and then excitation was switched to pulsed excitation at the same wavelength and average excitation power until photobleaching occurred. As can be seen in the autocorrelation curves, triplet formation is much more frequent in the pulsed excitation period compared to the CW excitation period. The average τ_t and Y_{tf} of g1r1 and g1r4 obtained by CW and pulsed excitation, respectively, for about 40 molecules

SCHEME 1: Photophysical Processes that Can Occur When Two Excited Chromophores Are Present

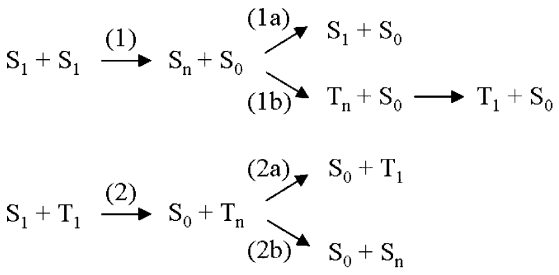

are depicted in the inset of Figure 7b. For g1r4, these values were calculated from the first intensity level in the trace. It can be seen that, for g1r4, the value of Y_{tf} calculated from the pulsed excitation period is 10 times higher than that calculated from the CW excitation period. The τ_t in the pulsed excitation period is slightly shorter than in the CW excitation period and is also shorter than that of g1r1. On the other hand, for g1r1, the influence of the excitation condition is small compared to g1r4. These results indicate that only the triplet parameters of this multichromophoric dendrimer are influenced under pulsed excitation conditions. As described above, it is possible to excite multiple chromophores at the same time by the use of pulsed excitation, whereas under CW excitation, the probability of exciting more than one chromophore is very low. It is clear, therefore, that multiple chromophore excitation plays an important role as an accessible photophysical pathway. We explain the increase of Y_{tf} and the decrease of τ_t with the number of chromophores by the mechanisms described in Scheme 1.

Although S_1-S_1 annihilation leading to a higher excited S_n (process 1 in Scheme 1) followed by a return to the S_1 state (process 1a in Scheme 1) is the main pathway, an additional pathway is opened where intersystem crossing from the higher excited singlet state S_n to T_n occurs (process 1b in Scheme 1), and this process leads to an increase of the triplet formation yield.[50]

Regarding the shortening of $\tau_{triplet}$ in g1r4 compared to g1r1, S_1-T_1 annihilation (process 2) likely plays an important role.[51] While process 2a is normal S_1-T_1 annihilation, process 2b, in which reverse intersystem crossing from T_n to S_n occurs, is also possible. Photoinduced reverse intersystem crossing has been demonstrated to be an effective mechanism for the shortening of the triplet lifetime at the single-molecule level.[27,52,53]

Influence of Stronger Interchromophoric Interaction on the Single-Photon Source. As described above, the interchromophoric interactions in g1r4 are of a weakly coupled nature. On the other hand, with an increasing number of chromophores in g1r8, interchromophoric interactions change to stronger coupling, that is, ground-state interactions exist due to the change of interchromophoric distances (Table 1). Here, we demonstrate the influence of such stronger interaction on single-photon sources by measuring g1r8 as a representative. As can be seen in Figure 2a, g1r8 shows a red-shifted, broad emission spectrum resulting from excimer-like emission indicating that stronger coupling between the chromophores exists in g1r8. The existence of this stronger interaction can be confirmed by measuring decay time traces of single g1r8 molecules. The time traces of the fluorescence intensity, the decay time, the N_C/N_L ratio, and the interphoton arrival time distribution of g1r8 embedded in zeonex are shown in Figure 8. It is evident that g1r8 shows decay times which fluctuate between 4 and 14 ns. Decay times longer than 4 ns are indicative of stronger coupling between the chromophores,[24,25] and the fluctuation of the decay time suggests that dynamic variations of the interchromophoric interactions exist in a single g1r8 molecule at room temperature. From the time trace of the N_C/N_L ratio and the interphoton arrival time distribution, it is clear that g1r8 also behaves as a single-photon emitter as a result of efficient S_1-S_1 annihilation. The Mandel parameters calculated from the first intensity levels of g1r8 (average of 50 molecules) under different conditions are shown in Table 3. Clearly, the efficiency as a single-photon emitter of g1r8 is lower than that of g1r4 despite the increase in the number of chromophores. This is remarkable because both dendrimers are cycled between the ground and the excited state under saturation conditions. Furthermore, the reduction in the efficiency caused by triplet blinking (the change of the Mandel parameter between zeonex under ambient atmosphere and under N_2 condition) is more pronounced than that for g1r4.

TABLE 3: Triplet Lifetime (τ_t), Triplet Formation Yield (Y_{tf}), and Mandel Parameter of g1r8, under Different Conditions (Embedded in PMMA under Ambient Condition and in Zeonex under N_2 Flow Condition Using Pulsed Excitation)[a]

compound	polymer	condition	τ_t (ms)	Y_{tf}	Mandel parameter (Q_s)
g1r8	PMMA	ambient	0.061	5×10^{-3}	−0.306
	zeonex	ambient			−0.466
	zeonex	N_2	0.043	6×10^{-3}	−0.298

[a] Each value was calculated from the first intensity level of their fluorescence time traces as the average value of 50 individual molecules. The detection efficiency was taken into account as 5%.

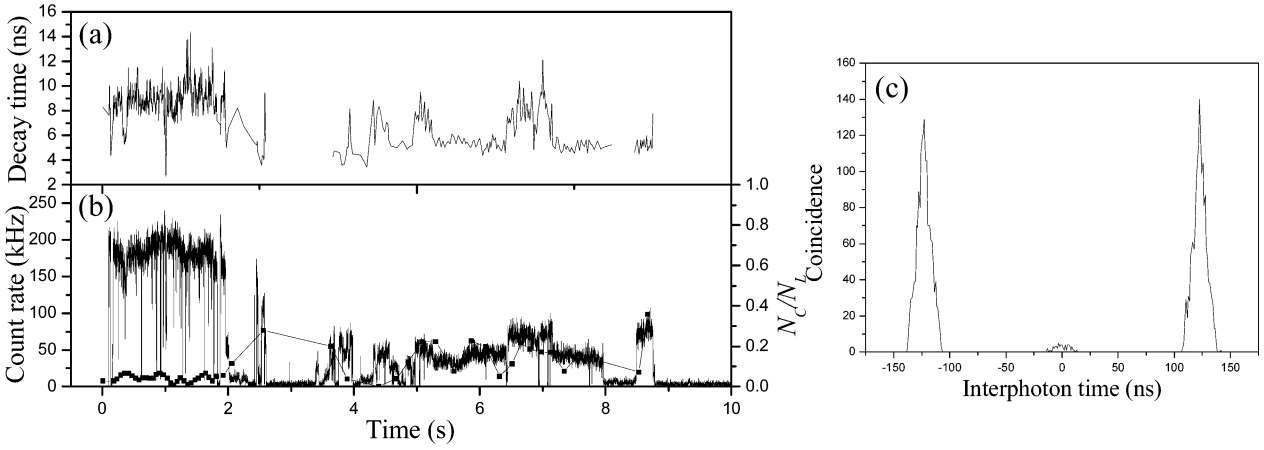

Figure 8. Time traces of fluorescence intensity (b, solid line), fluorescence decay time (a), and N_C/N_L ratio (b, square) measured from a single g1r8 embedded in zeonex. (c) Interphoton arrival time distribution obtained from the first fluorescence intensity level of the time trace b.

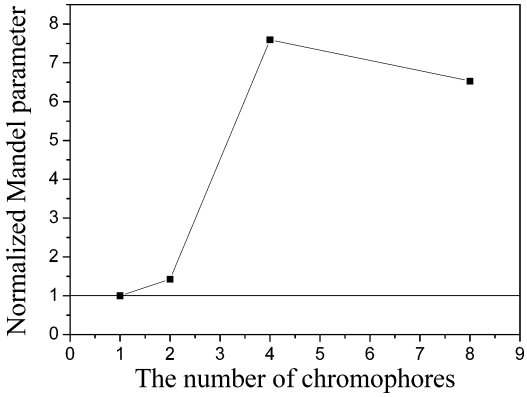

Figure 9. Normalized Mandel parameter (normalized to g1r1) for g1r1, g1r2, g1r4, and g1r8. The different compounds were measured in similar conditions: 3 μW pulsed excitation, embedded in zeonex, and in ambient condition.

Although the excimer-like species exhibits a lower fluorescence quantum yield compared to the locally excited state of perylenemide, the influence of stronger coupling between chromophores on intersystem crossing and the triplet lifetime as described below needs to be considered as well to understand the change of the single-photon source efficiency.

As predicted by exciton splitting theory, stronger coupling between two chromophores and subsequent exciton splitting creates an energetically lower state which is closer to the triplet state as compared to the original state.[54−56] It is considered that this splitting can result in a higher frequency of intersystem crossing. Average values of Y_{tf} and τ_t from the first intensity level of individual g1r8 molecules embedded in PMMA under ambient conditions and in zeonex under N_2 flow are shown in Table 3. Interestingly, the value of Y_{tf} determined from g1r8 is higher than the value from g1r4: Y_{tf} (g1r8) > Y_{tf} (g1r4). To see if this is due to a higher frequency of process 1b in g1r8 compared to g1r4 or due to stronger interactions, a CW excitation experiment was performed under similar conditions. The value of Y_{tf} for CW excitation equals 4×10^{-3}, indicating that the rate of intersystem crossing for S_1 to T_1 is substantially increased, obscuring the effect of pulsed excitation.

Y_{tf} estimated from the CW excitation period is much higher than that from the CW excitation period in g1r4 (see Figure 7b). This increase indicates the influence of exciton splitting in g1r8. From the above results, it is clearly shown that the number of chromophores and the occurrence of stronger coupling influences the triplet formation yield, such that (1) if all chromophores are weakly coupled (Förster regime), Y_{tf} increases with an increasing number of chromophores (influence of process 1b) and (2) if a stronger interchromophore coupling exists, Y_{tf} increases further as a result of exciton splitting.

Here, we summarize the decay pathways of g1r4 (weak coupling) and g1r8 (stronger coupling). In the case of g1r4, as described above, after multiple chromophore excitation, in almost all cases, S_1-S_1 annihilation occurs resulting in a single S_n being formed, which then decays to S_1 which emits or seldomly undergoes intersystem crossing Y_{tf} (10^{-5}). In addition to this intersystem crossing, process 1b also occurs, and this process leads to an increase of the Y_{tf} (10^{-4}). As a result, T_1 is formed. Then, when other chromophores are excited by the excitation pulse within the decay time of T_1, S_1 and T_1 now exist in a single dendrimer, and efficient (efficiency is almost 100%) S_1-T_1 annihilation occurs. T_n states formed as a result of S_1-T_1 annihilation can undergo reverse intersystem crossing to S_n (process 2b), yielding a shortening of τ_t.

In the case of g1r8 (stronger coupling), S_1-S_1 annihilation also occurs in the same manner as for g1r4. However, the energetically lower S_1, split by interaction energy, is closer to the triplet state, and, thus, more efficient intersystem crossing occurs in addition to g1r4 (process 1b). Subsequently, S_1 is formed upon excitation and S_1-T_1 annihilation occurs in the same manner as g1r4. It is expected, however, that the frequency of S_1-T_1 annihilation increases with an increasing number of

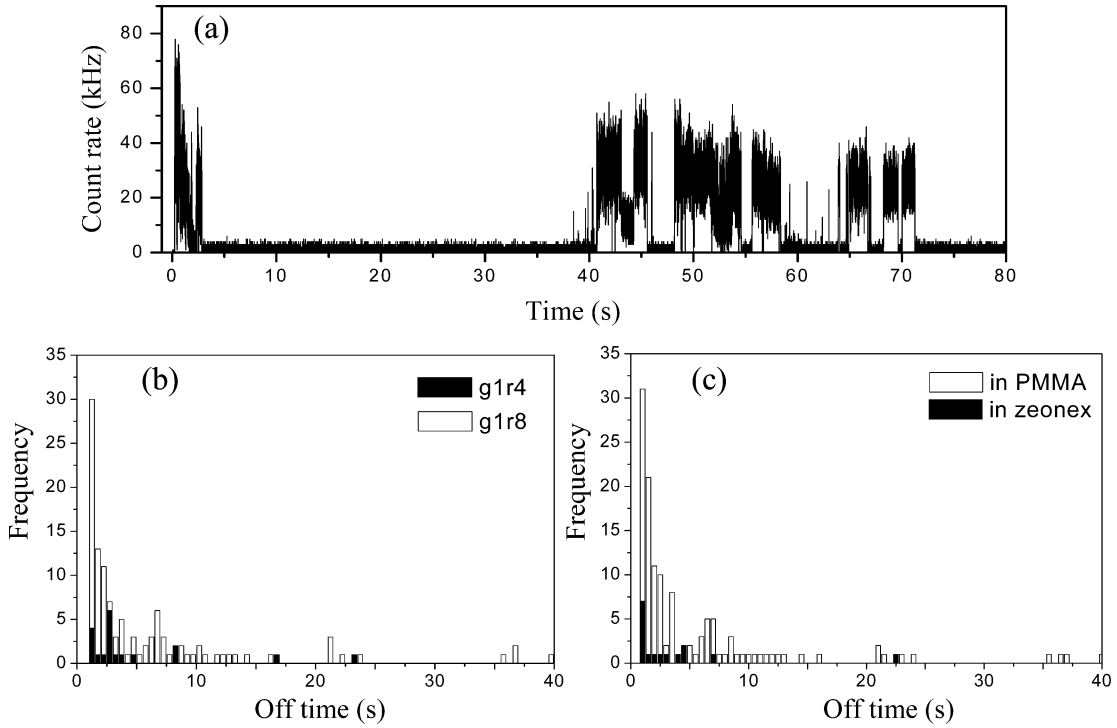

Figure 10. (a) Fluorescence intensity time trace of g1r8 embedded in PMMA. A long off state can be seen ranging from 3 to 38 s. (b) Histogram of the long off times (>1 s) measured from single g1r4 and g1r8 embedded in PMMA. (c) Histogram of the long off times measured from single g1r8 embedded in PMMA and in zeonex under ambient conditions.

chromophores, resulting in further shortening of τ_t in g1r8 compared to that in g1r4. In addition, the splitting of the energy level of g1r8 enables a higher efficiency of reverse intersystem crossing (process 2b) compared to g1r4 as a result of better matching of singlet and triplet energy levels and/or relaxation of the symmetry restriction; thus, we speculate that this is one possibility of shortening of τ_t in g1r8. In Figure 9 the single-photon source efficiency is given by normalizing the Mandel parameters of g1r1, g1r2 (the value of g1r2 was determined from data in the literature),[21] g1r4, and g1r8 to g1r1. One can see that at 3-μW excitation power, a maximum can be seen at g1r4, indicating that this is the most efficient single-photon source at these experimental conditions.

Influence of the Long Off Time on These Single-Photon Sources. Depending on the time scale of the off state, different kinds of nonradiative traps have been taken into consideration.[21] Triplet blinking is one of them, and in this case, the time scale of the off state ranges from a few tens of microseconds to about 1 ms, as mentioned above. For longer off states of several milliseconds duration, singlet−radical ion interactions have been proposed.[21,57] The multichromophoric dendrimers, however, sometimes show even much longer off states up to tens of seconds. A fluorescence intensity time trace measured from g1r8 embedded in PMMA, which includes such a long off state, is shown in Figure 10a. In this trace, a long off time of about 35 s duration can be seen. It was found that the frequency and off time of the long off state depends strongly on the number of chromophores and the polymer matrix. Figure 10b shows a histogram of the long off times (longer than 1 s) measured for dendrimers with different numbers of chromophores embedded in PMMA.

It can be seen that the frequency and off-time increase with increasing the number of chromophores. A total of 69% of the g1r8 molecules and 55% of the g1r4 molecules showed such a long off state. The histograms of the long off times of g1r8 embedded in PMMA and zeonex are shown in Figure 10c, and the dependence on the nature of the polymer matrix can be seen clearly. In zeonex, 43% of the molecules showed the long off state, which is less frequent compared to PMMA. Thus, it is considered that an oxygen-adduct[31] which acts as a quencher of fluorescence is probably excluded as long off periods are occurring with high frequency in PMMA. This long collective off state is an undesirable phenomenon for a single-photon source; therefore, it is concluded that dendrimers with a small number of chromophores embedded in zeonex are better for inhibiting the long off state and for realizing an efficient single-photon source at low excitation power. However, for the determination of the Mandel parameter of the different compounds in this paper, this effect did not play any role because the analysis was done on the first, highest intensity level and these long collective off states appear later in the transient.

Conclusions

In this article we have investigated the parameters which influence the efficiency of multichromophoric dendrimers as single-photon sources by measuring the fluorescence intensity, the fluorescence decay time, and the interphoton arrival time distribution simultaneously. It has clearly been shown that all measured first-generation multichromophoric dendrimers behave as a single-photon emitter regardless of the number of chromophores, even when more than two chromophores are excited by single excitation pulse. Whether or not the multichromophoric dendrimers act as single-photon sources depends on the S_1-S_1 annihilation efficiency as was demonstrated by comparing g1r4 with eg1r4. On the other hand, the efficiency as a single-photon source depends on several parameters, such as the nature of the surrounding polymer matrix, the number of chromophores, and the interchromophoric interaction. Under a high oxygen concentration like in zeonex, which has high oxygen permeability and solubility, shortening of the triplet decay time as a result of quenching of the triplet state by oxygen leads to a higher efficiency as a single-photon source, while photobleaching for this chromophore is much less of an issue. It was demonstrated that in the multichromophoric dendrimers in which interchromophoric interaction is limited to weak coupling, the increase of Y_{tf} as a result of an additional intersystem crossing from a higher excited single state influences the efficiency as a single-photon source. Furthermore, in multichromophoric dendrimers which have stronger coupling between chromophores, the splitting of the locally excited state resulted in a further increase of Y_{tf} in addition to intersystem crossing from a higher excited singlet state. This further decreases the efficiency of strongly coupling dendrimers as single-photon sources. Therefore, we conclude that a multichromophoric system with weakly coupled interchromophoric interactions in the presence of an adequate triplet quencher is the most promising single-photon source because it can be operated at low excitation power, optimizing the signal-to-background ratio. In this work, g1r4 is classified as such a multichromophoric system. Nevertheless, organic dyes can for the moment not compete with the inorganic single-photon sources such as nanocrystals, quantum dots, or color centers in diamonds which have a much larger photostability.

Acknowledgment. S.M. and T.D.M.B. gratefully acknowledge KU Leuven for postdoctoral fellowships. Financial support of FWO, the Federal Science Policy through IUAP-5-30, the Flemish Ministry of Education through GOA/1/2001, the German Federal Ministery of Technology, the German Science Foundation, and a Max Planck research award are gratefully acknowledged. B.C. thanks the Belgian National Fund for Scientific Research for his Senior Research Associate fellowship. D.B. is a Senior Research Associate of the Belgian National Science Foundation (FNRS).

References and Notes

(1) Meystre, P.; Sargent, M. *Elements of Quantum Optics*; Springer: Berlin, 1990.
(2) Drummond, P. D. *Quantum Squeezing*; Springer: Berlin 1999.
(3) Gisin, N.; Ribordy, G. G.; Tittel, W.; Zbinden, H. *Rev. Mod. Phys*. **2002**, *74*, 145.
(4) Bennett, C. H.; Brassard, G.; Ekert, A. K. *Sci. Am*. **1992**, *267*, 50.
(5) Benett, C. H.; Brassard, G.; Mermin, N. D. *Phys. Rev. Lett*. **1992**, *68*, 557.
(6) Turchette, Q. A.; Hood, C. J.; Lange, W.; Mabuchi, H.; Kimble, H. J. *Phys. Rev. Lett*. **1995**, *75*, 4710.
(7) Kimble, H. J.; Dagenais, M.; Mandel, L. *Phys. Rev. Lett*. **1977**, *39*, 691.
(8) Solomon, G. S.; Pelton, M.; Yamamoto, Y. *Phys. Rev. Lett*. **2001**, *86*, 3903.
(9) Santori, C.; Pelton, M.; Solomon, G.; Dale, Y.; Yamamoto, Y. *Phys. Rev. Lett*. **2001**, *86*, 1502.
(10) Kim, J.; Benson, O.; Kan, H.; Yamamoto, Y. *Nature* **1999**, *397*, 500.
(11) Yuan, Z.; Kardynal, B. E.; Stevenson, R. M.; Shields, A. J.; Lobo, C. J.; Cooper, K.; Beattie, N. S.; Ritchie, D. A.; Pepper, M. *Science* **2002**, *295*, 102.
(12) Basché, T.; Moerner, W. E.; Orrit, M.; Talon, H. *Phys. Rev. Lett.* **1992**, *69*, 1516.
(13) Brunel, C.; Lounis, B.; Tamarat, P.; Orrit, M. *Phys. Rev. Lett*. **1999**, *83*, 2722.
(14) Beveratos, A.; Brouri, R.; Gacoin, T.; Poizat, J.-P.; Grangier, P. *Phys. Rev. A* **2001**, *64*, 061802(R).
(15) Michler, P.; Imamoğlu, A.; Mason, M. D.; Carson, P. J.; Strouse, G. F.; Buratto, S. K. *Nature* **2000**, *406*, 968.

(16) Tinnefeld, P.; Weston, K. D.; Vosch, T.; Cotlet, M.; Weil, T.; Hofkens, J.; Müllen, K.; De Schryver, F. C.; Sauer, M. *J. Am. Chem. Soc.* **2002**, *124*, 14310.

(17) Tinnefeld, P.; Müller, C.; Sauer, M. *Chem. Phys. Lett*. **2001**, *345*, 252.

(18) Treussart, F.; Alléaume, R.; Le Floc'h, V.; Xiao, L. T.; Courty, J.-M.; Roch, J.-F. *Phys. Rev. Lett*. **2002**, *89*, 093601-1.

(19) Lounis, B.; Moerner, W. E. *Nature* **2000**, *407*, 491.

(20) Lill, Y.; Hecht, B. *Appl. Phys. Lett.* **2004**, *84*, 1665.

(21) Vosch, T.; Cotlet, M.; Hofkens, J.; Van Der Biest, K.; Lor, M.; Weston, K. D.; Tinnefeld, P.; Sauer, M.; Latterini, L.; Müllen, K.; De Schryver, F. C. *J. Phys. Chem. A* **2003**, *107*, 6920.

(22) Ying, L.; Xie, X. S. *J. Phys. Chem. B* **1998**, *102*, 10399−10409.

(23) Hofkens, J.; Schroeyers, W.; Loos, D.; Cotlet, M.; Köhn, F.; Vosch, T.; Maus, M.; Herrmann, A.; Müllen, K.; Gensch, T.; De Schryver, F. C. *Spectrochim. Acta, Part A* **2001**, *57*, 2093.

(24) Vosch, T.; Hofkens, J.; Cotlet, M.; Köhn, F.; Fujiwara, H.; Gronheid, R.; Van Der Biest, K.; Weil, T.; Herrmann, A.; Müllen, K.; Mukamel, S.; Van der Auweraer, M.; De Schryver, F. C. *Angew. Chem., Int. Ed.* **2001**, *40*, 4643.

(25) Hofkens, J.; Maus, M.; Gensch, T.; Vosch, T.; Cotlet, M.; Köhn, F.; Herrmann, A.; Müllen, K.; De Schryver, F. C. *J. Am. Chem. Soc*. **2000**, *122*, 9278.

(26) Hofkens, J.; Cotlet, M.; Vosch, T.; Tinnefeld, P.; Weston, K. D.; Ego, C.; Grimsdale, A.; Müllen, K.; Beljonne, D.; Brédas, J. L.; Jordens, S.; Schweizer, G.; Sauer, M.; De Schryver, F. C. *Proc. Natl. Acad. Sci. U.S.A.* **2003**, *100*, 13146.

(27) Tinnefeld, P.; Buschmann, V.; Weston, K. D.; Sauer, M. *J. Phys. Chem. A* **2003**, *107*, 323.

(28) Bopp, M. A.; Sytnik, A.; Howard, T. D.; Cogdell, R. J.; Hochstrasser, R. M. *Proc. Natl. Acad. Sci. U.S.A.* **1999**, *96*, 11271.

(29) Bopp, M. A.; Jia, Y. W.; Li, L. Q.; Cogdell, R. J.; Hochstrasser, R. M. *Proc. Natl. Acad. Sci. U.S.A.* **1997**, *94*, 10630.

(30) Cotlet, M.; Hofkens, J.; Habuchi, S.; Dirix, G.; Van Guyse, M.; Michiels, J.; Vanderleyden, J.; De Schryver, F. C. *Proc. Natl. Acad. Sci. U.S.A.* **2001**, *98*, 14398.

(31) Yu, J.; Hu, D. H.; Barbara, P. F. *Science* **2000**, *289*, 1327.

(32) Vanden Bout, D.; Yip, W. T.; Hu, D. H.; Fu, D. K.; Swager, T. M.; Barbara, P. F. *Science* **1997**, *277*, 1074.

(33) Bussian, D. A.; Summers, M. A.; Liu, B.; Bazan, G. C.; Buratto, S. K. *Chem. Phys. Lett.* **2004**, *288*, 181.

(34) Weil, T.; Wiesler, U. M.; Herrmann, A.; Müllen, K. *J. Am. Chem. Soc.* **2001**, *123*, 8101.

(35) Morgenroth, F.; Kübel, C.; Muller, M.; Wiesler, U. M.; Berresheim, A. J.; Wagner, M.; Müllen, K. *Carbon* **1998**, *36*, 833.

(36) Morgenroth, F.; Berresheim, A. J.; Wagner, M.; Müllen, K. *Chem. Commun*. **1998**, 1139.

(37) Morgenroth, F.; Reuther, E.; Müllen, K. *Angew. Chem., Int. Ed. Engl*. **1997**, *36*, 631.

(38) Morgenroth, F.; Müllen, K. *Tetrahedron* **1997**, *53*, 15349. The synthesis of g1r8 will be published separately.

(39) Parr, R. G.; Yang, W. *Density-Functional Theory of Atoms and Molecules*; Oxford University Press: Oxford, 1989.

(40) Becke, A. D. *J. Chem. Phys.* **1993**, *98*, 5648.

(41) Hanbury-Brown, R.; Twiss, R. *Nature* **1956**, *177*, 27.

(42) Weston, K. D.; Dyck, M.; Tinnefeld, P.; Müller, C.; Herten, D. P.; Sauer, M. *Anal. Chem*. **2002**, *74*, 5342.

(43) Maus, M.; De, R.; Lor, M.; Weil, T.; Mitra, S.; Wiesler, U.-M.; Herrmann, A.; Hofkens, J.; Vosch, T.; Müllen, K.; De Schryver, F. C. *J. Am. Chem. Soc.* **2001**, *123*, 7668.

(44) Jordens, S.; De Belder, G.; Lor, M.; Schweitzer, G.; Van der Auweraer, M.; Weil, T.; Herrmann, A.; Wiesler, U. K.; Müllen, K.; De Schryver, F. C. *Photochem. Photobiol. Sci*. **2003**, *2*, 1118.

(45) De Belder, G.; Schweitzer, G.; Jordens, S.; Lor, M.; Mitra, S.; Hofkens, J.; De Feyter, S.; Van der Auweraer, M.; Herrmann, A.; Weil, T.; Müllen, K.; De Schryver, F. C. *ChemPhysChem* **2001**, *2*, 49.

(46) Short, R.; Mandel, L. *Phys. Rev. Lett.* **1983**, *51*, 384.

(47) Mandel, L. *Opt. Lett.* **1979**, *4*, 205.

(48) *Polymer Handbook*, 3rd ed.; Brandrup, J. B., Immergat, E. H., Eds.; John Wiley and Sons, Inc.: New York, 1989; p 437.

(49) Weston, K. D.; Carson, P. J.; Metiu, H.; Buratto, S. K. *J. Chem. Phys.* **1998**, *109*, 7474.

(50) Tinnefeld, P.; Hofkens, J.; Herten, D.-P.; Masuo, S.; Vosch, T.; Cotlet, M.; Habuchi, S.; Müllen, K.; De Schryver, F. C.; Sauer, M. *ChemPhysChem*, accepted.

(51) Hübner, C. G.; Zumofen, G.; Renn, A.; Herrmann, A.; Müllen, K.; Basché, T. *Phys. Rev. Lett*. **2003**, *91*, 093903-1.

(52) English, D. S.; Harbron, E. J.; Barbara, P. F. *J. Phys. Chem. A* **2000**, *104*, 9057.

(53) Fleury, L.; Segura, J. M.; Zumofen, G.; Hecht, B.; Wild, U. P. *Phys. Rev. Lett.* **2000**, *84*, 1148−1151.

(54) McRae, M. G.; Kasha, M. **1958**, *28*, 721.

(55) Siebrand, W. *J. Chem. Phys.* **1966**, *44*, 4055.

(56) Twenty-five percent of the individual g1r8 molecules emit from a locally excited state of the peryleneimide chromophore (decay times were below 5 ns) and not from an excimer-like state even in the first intensity level. These g1r8 molecules were not considered in this paper.

(57) Zondervan, R.; Kulzer, F.; Orlinskii, S. B.; Orrit, M. *J. Phys. Chem. A* **2003**, *107*, 6770−6776.